Summary of Results from the Beam Sweep Test Module

F. M. Bieniosek
1-June-95

This report describes the measurements that were performed with the beam sweep test module on May 16, 1995. The main purpose of the experiment was to measure current draw between biased plates in air across the beam path downstream of the target. Additional data was taken from instrumented cores in the test module. The module was installed directly downstream of the collection lens module.

As the intensity of beam on target increases, it becomes necessary to blow up the beam spot on target to maintain peak energy deposition intensity on target below that which can be sustained by the target in routine operation (about 600 J/g for nickel). Unfortunately increasing the radial beam size also reduces the yield of antiprotons from the target. In order to maintain the yield from the target, we would like to sweep a tightly-focused beam on target on the time scale of the beam pulse. This kind of sweeping requires high currents (about 6 kA) on electrodes close to the beam path, and associated high inductive electric fields (about 6 kV across the magnet). Concern about the current drawn across the inductive electric field through air ionized by the shower of particles downstream of the target provided the impetus for this experiment.

The sweep magnet test piece consisted of a pair of copper plates (3 cm wide x 3 cm gap) centered on the incident beam. The high voltage conductors are insulated in torlon at all places except at the gap between the plates where the beam passes. The length of the conductors is 9.5 inch, but 1 inch of the length of the bars was insulated with kapton tape to ensure that breakdown could not occur to the collection lens water-cooling lines, which extend beyond the downstream edge of the lens module. Surrounding the plates are 5 magnetic cores - 2 pairs of ferrite cores from Ceramic Magnetics (CMD-10 and MN-67) with dimensions 6 cm ID, 12 cm OD, 2.54 cm height, and a single

tape-wound core (Magnetic Metals P/N 201P4601) which consists of a .001-inch 50% nickel/iron "Square 50" tape of core dimensions 3-inch ID, 4.5-inch OD and 1.5-inch height. Net core area=5.444 cm^2 and mean path length = 29.92 cm. The cores are instrumented with thermocouples at the inner and outer radii, and by a winding of 100 turns of 20-ga magnet wire for measurement of short-term radiation effects on the cores. The entire assembly is mounted in an aluminum box and hangs from a blank target module by means of a special-design hanging fixture. The module was surveyed and centered on the beam transversely to within 0.005 inch. A photograph of the magnet test piece is show in Figure 1. Since no provision was made for remote disconnect of the module, it was necessary to minimize the number of pulses seen by the module. In the experiment, 31 beam pulses were used.

The circuit used to bias the plates is shown in Figure 2. A bipolar pair of high voltage supplies are used to charge up a pair of 0.15-μF capacitors. Two RG-8 cables connect these capacitors to the plates. The effective length of the cables is 100 ns; because two cables are used in the circuit, the effective impedance of the circuit is 100 Ω. The current supplied to the plates is measured by a Pearson current monitor at the power supply end of the cable. When a beam pulse occurs, it ionizes the air downstream of the lens, and the conductivity of the ionized air completes the circuit. Low-voltage tests with an SCR switch across the gap showed that a resistance as low as 10 Ω can be measured with this circuit on a 1.6-μs time scale.

Figure 3 shows current pulses for two beam intensities with the same voltage drop across the gap (10 kV, +5 kV on one plate, -5 kV on the other plate). The scope bandwidth for the measurements shown here is 20 MHz. The current rises quickly (rise time less than 100 ns) and comes to equilibrium after a small initial reflection in the cable. The effective resistance of the ionized air is slightly larger than 100 Ω. The flattop in the current pulse shows some droop because of the loss of charge of the capacitor during the pulse (voltage loss during the pulse is approximately 10-15%). The air deionizes quickly after the end of the beam pulse (fall time less than 100 ns), and large oscillations occur because the cable is mismatched at both ends when the gap is open. Note that a large inductive transient voltage is expected across the gap at the moment of turn-off of the gap - the magnitude of the inductive drop is the product of the interrupted current times the effective impedance of the circuit. This voltage spike adds to the DC voltage applied across the gap. The fact that the current is quickly interrupted is the clearest evidence that the gap did not break down. Figure 4 shows the current pulses for the largest gap voltages. In this case the additional inductive voltage spike of over 10 kV fails to break down the gap. The scope bandwidth for these measurements is 250 MHz. Figure 5 is a plot of the peak measured leakage current as a function of supply voltage for two different beam intensities. The

fact that the data do not fall in straight line is a reflection of the fact that the conductivity of a plasma depends on the electron mobility, which is a function of the electric field. One of the data points represents 10 pulses at 12 kV and 2.6×10^{12} protons/pulse, indicating very little jitter in the leakage current measurement. There is again no sign of avalanche breakdown, which would be apparent as a rapid buildup of current to the maximum level that can be supplied by the circuit, in this case over 1 kA. Avalanche breakdown is not expected to occur until the electric field significantly exceeds 10 kV/cm, *i.e.* well over 30 kV in this case.

Agreement with the prediction (resistance of 50 Ω at an intensity of 5×10^{12}) of a plasma model of the ionized air is fairly good [1]. This agreement is somewhat fortuitous because of the nature of the approximations involved in the calculation. In particular the calculation was for an inductive electric field distribution, which is somewhat different from the DC field distribution of this test. In addition, the model was based on a simple balance between source (by ionization) and loss (by recombination) of the plasma electrons. Other processes, such as electron attachment on oxygen and water vapor molecules in the air are likely to have a major effect in reducing the conductivity of the air. These two inaccuracies in the model appear to have roughly canceled each other out. The theoretical scaling of plasma conductivity with beam intensity should be proportional to the square root of the intensity; the data show a slightly stronger dependence.

Thermocouple data for a 10-pulse test is shown in Figure 6. A summary of the data is contained in Table 1. The MN-67 cores are at the upstream location in the test piece. The beam intensity is 2.6×10^{12} protons/pulse.

Table I

	IN	OUT
MN-67	0.19 deg-C	0.11 deg-C
tape-wound	0.19	0.10
CMD-10	0.16	0.08

The specific heat of MnZn ferrite (MN-67) is 1.1 J/g/C, and the specific heat of NiZn ferrite (CMD-10) is 0.75 J/g/C. The results agree within about a factor of two with the thermal heating predicted by CASIM calculations.

Finally, measurements were made of the effect of the beam pulse on the magnetic cores. The purpose of this measurement is to determine any short-term radiation effect on the magnetic properties of the material. This

measurement is particularly important in ferrite, because the sweep magnet operates near the saturation field of ferrite material. An instantaneous drop in the saturation flux level could directly affect the magnetic field in the gap. The magnets were biased with about 1 A flowing through the 100-turn windings. This bias places the cores near saturation. When a rapid change in the flux ϕ in the core, due to a change in the saturation flux level, occurs, a current i appears in the winding, given by

$$\frac{d\phi}{dt} = iR + L\frac{di}{dt}$$

where R and L are the resistance and inductance of the circuit. For $L>>Rt$, which is appropriate for the conditions of this measurement with a 50-Ω impedance at the scope, we have a simple expression relating the change of flux to the measured change in current

$$\Delta\phi = L\,\Delta i$$

or

$$\Delta B = \frac{L}{A}\frac{\Delta V}{50\,\Omega}$$

where A is the cross-sectional area of the core. All the measurements were taken through 20 dB (factor-of-10) attenuators, so that for the ferrite cores, ΔB=1 Gauss/mV. Figure 7 shows the results for two cores. The results are plotted as the difference in signal between biased and unbiased cases, to cancel out some of the noise. The noise appears to come from coupling of the high-current pulse in the high voltage circuit to the signal cables. In addition the windings on the cores oscillate at a self-resonant frequency of a few MHz. The wandering behavior on a 5-μs time scale is only observed when the cores are biased. It is tentatively identified as a short-term radiation effect. Significant signals occurred from the MN-67 cores (ΔB = about -100 Gauss). The CMD-10 cores showed a small effect in the opposite direction than the MN-67, and the tape-wound cores showed almost no effect. The signals were not due to pickup of any net current due to the beam because the ferrite cores were installed in pairs, and wound in opposite directions. The sign of the signals was the same for each core of a pair.

[1] F. M. Bieniosek, A beam sweeping system for the Fermilab Antiproton Production Target, Fermilab-TM-1857 (1993).

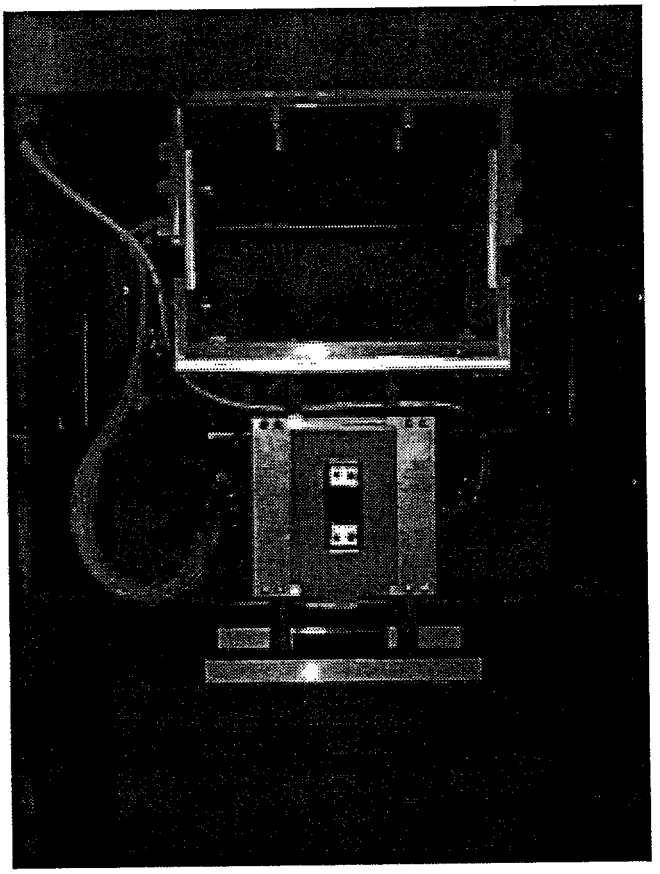

Fig. 1

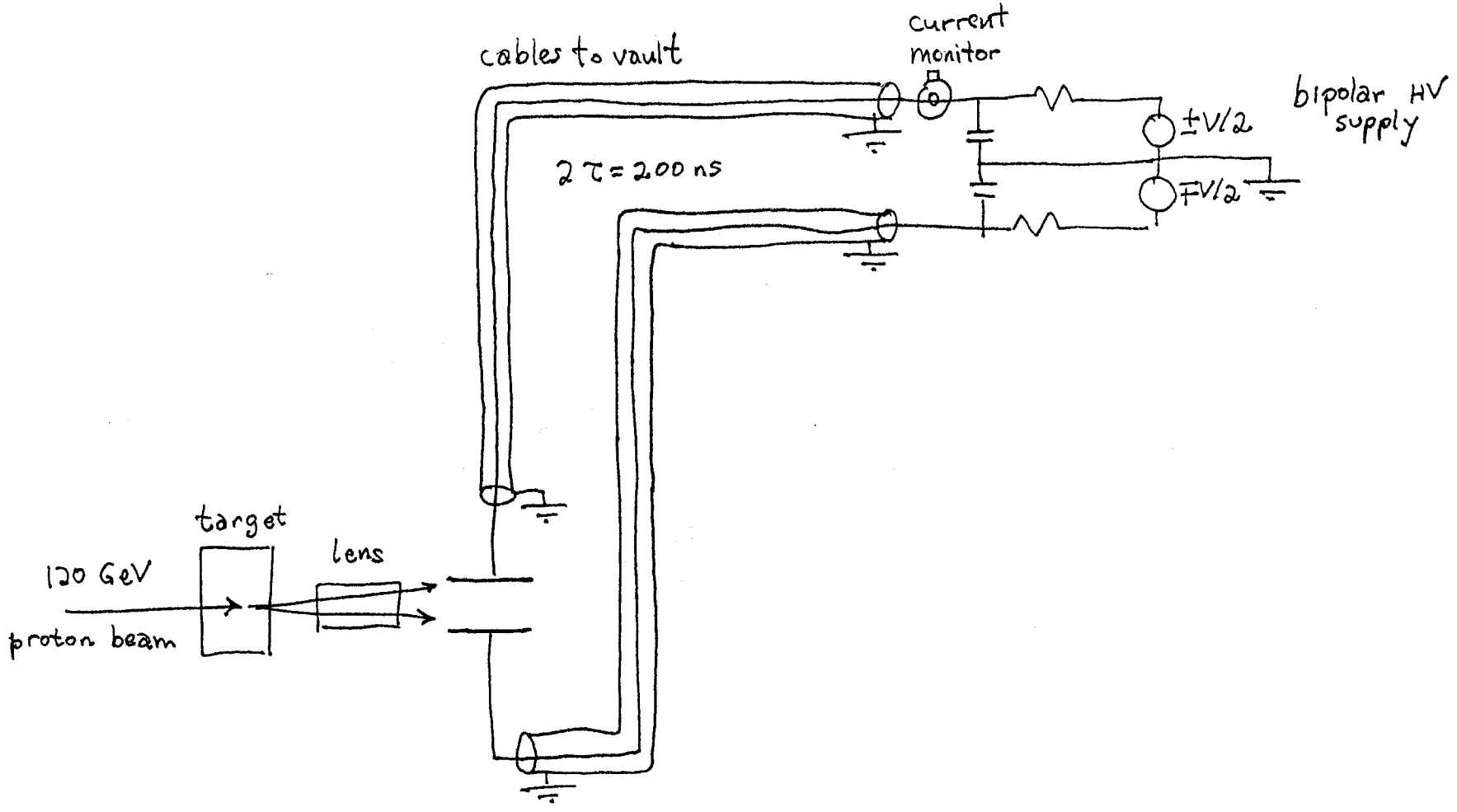
cables to vault
current monitor
bipolar HV supply
±V/2
∓V/2
2τ = 200 ns
target
lens
120 GeV
proton beam

Fig. 2

Figure 3.
Beam sweep test: ΔV_{supply} = 10 kV

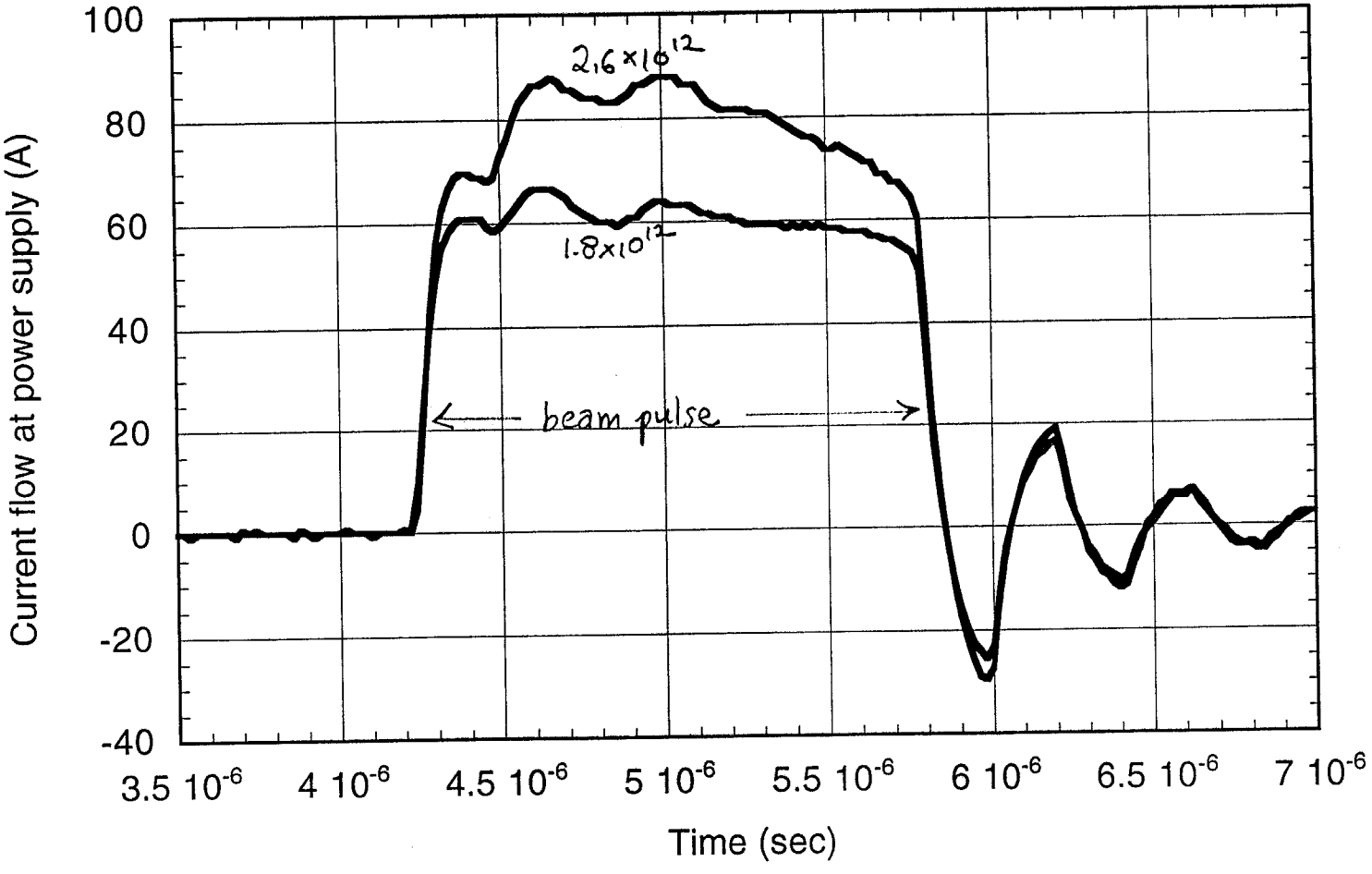

Figure 4
Beam sweep test: 2.6e12 protons/pulse

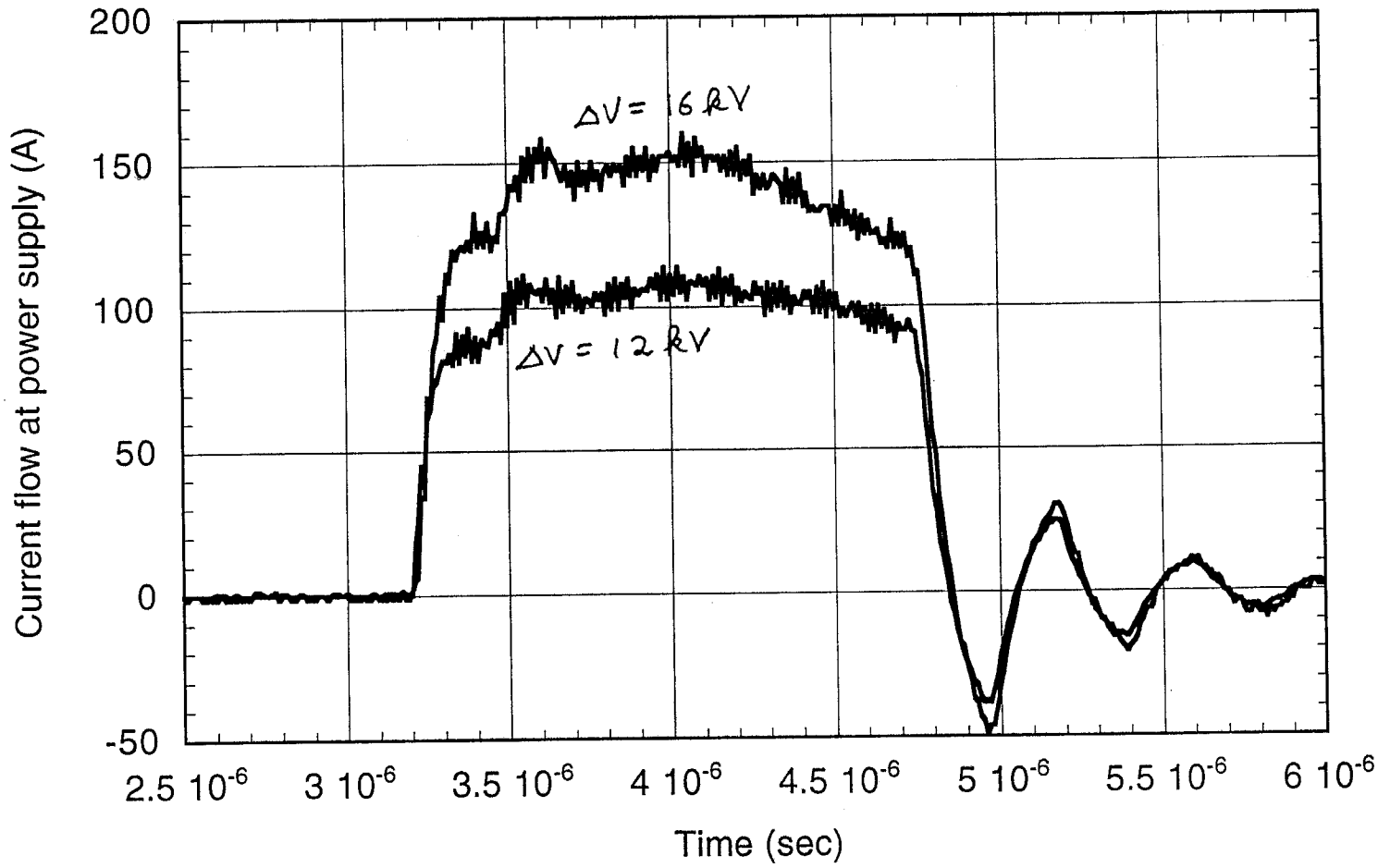

Figure 5.
Scaling of current with voltage and beam intensity

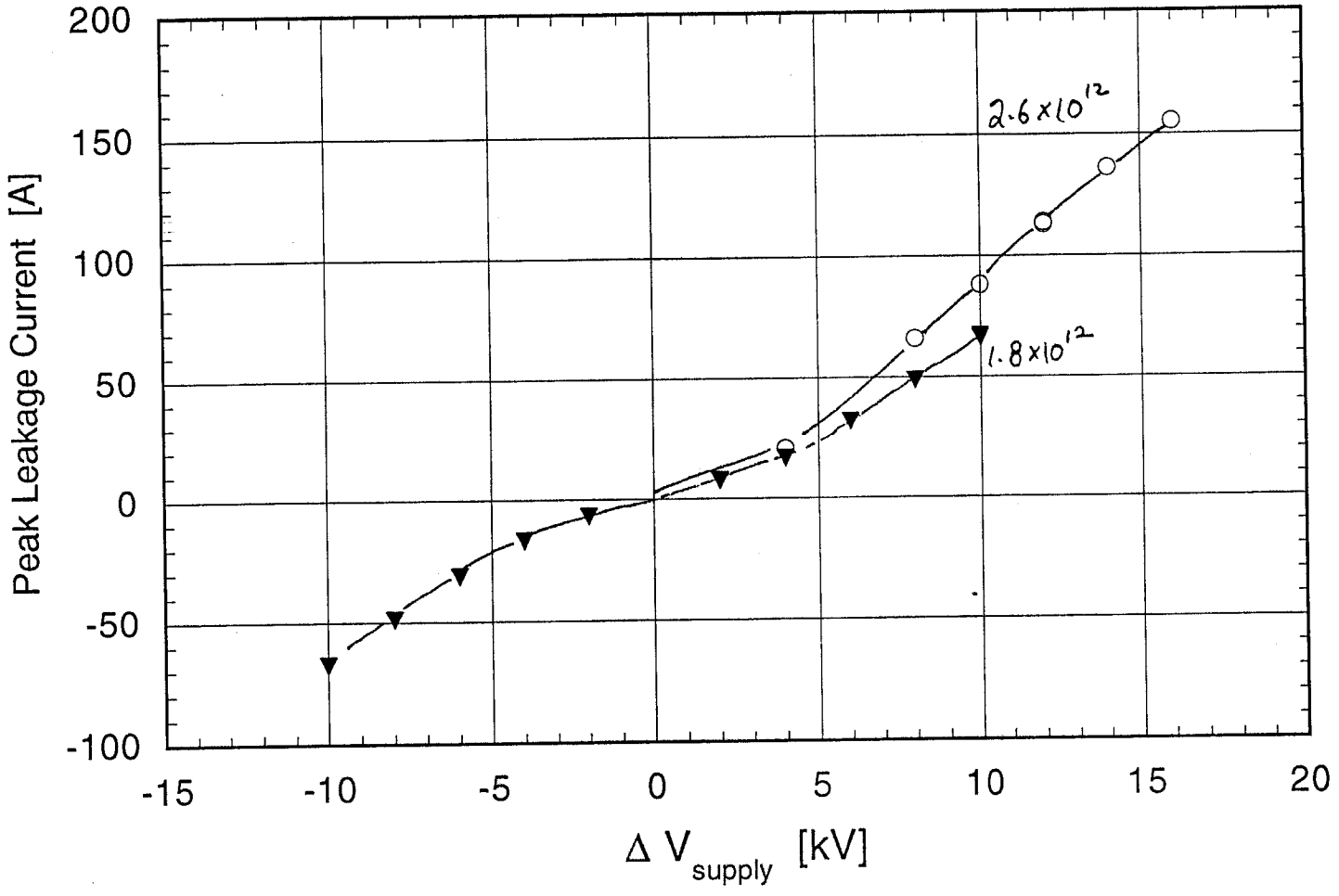

Prototype Sweep Magnet Core Temperatures

Ten Pulse Beamline Test; Intensity = 2.5 x 10E12

May 16, 1995

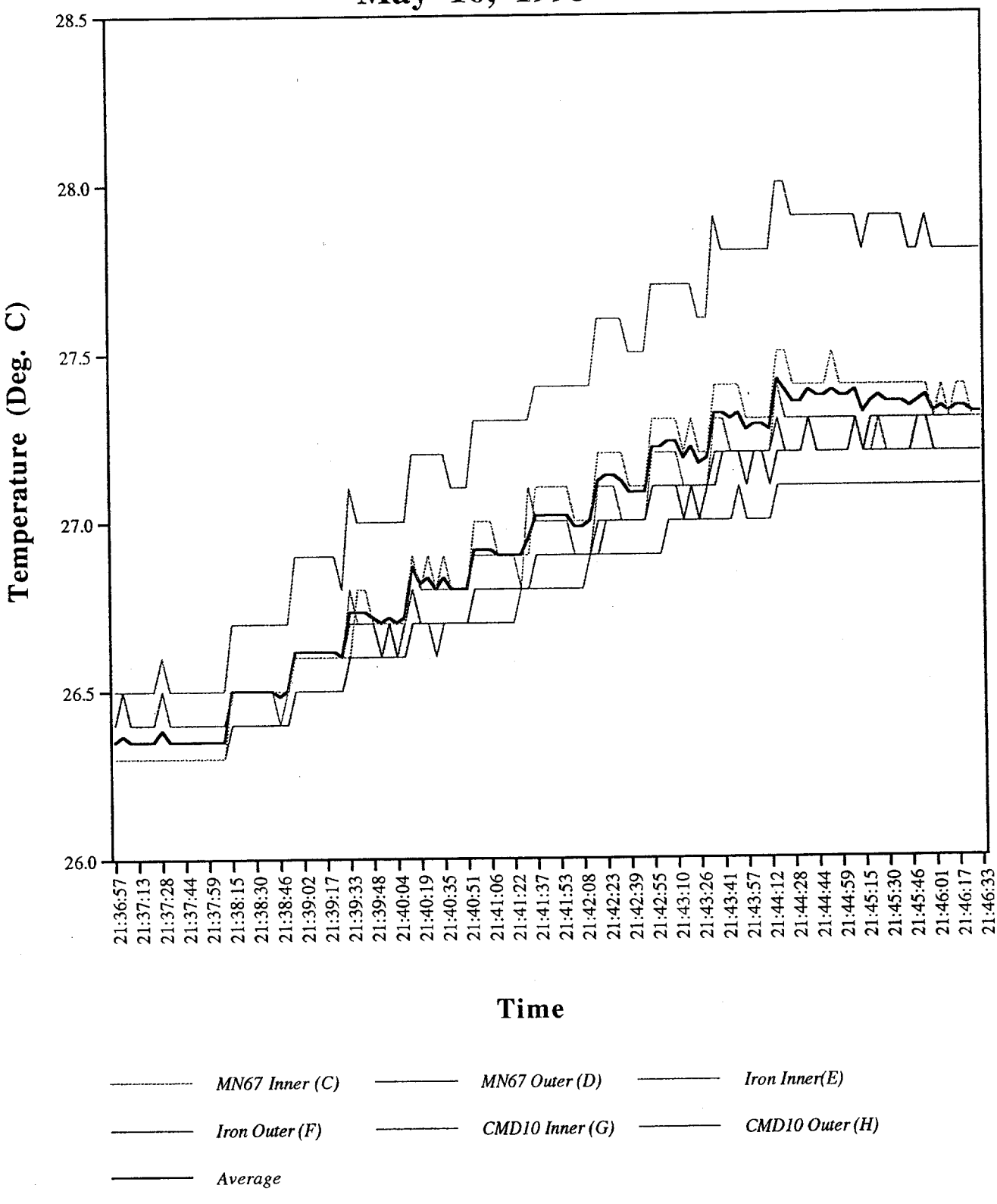

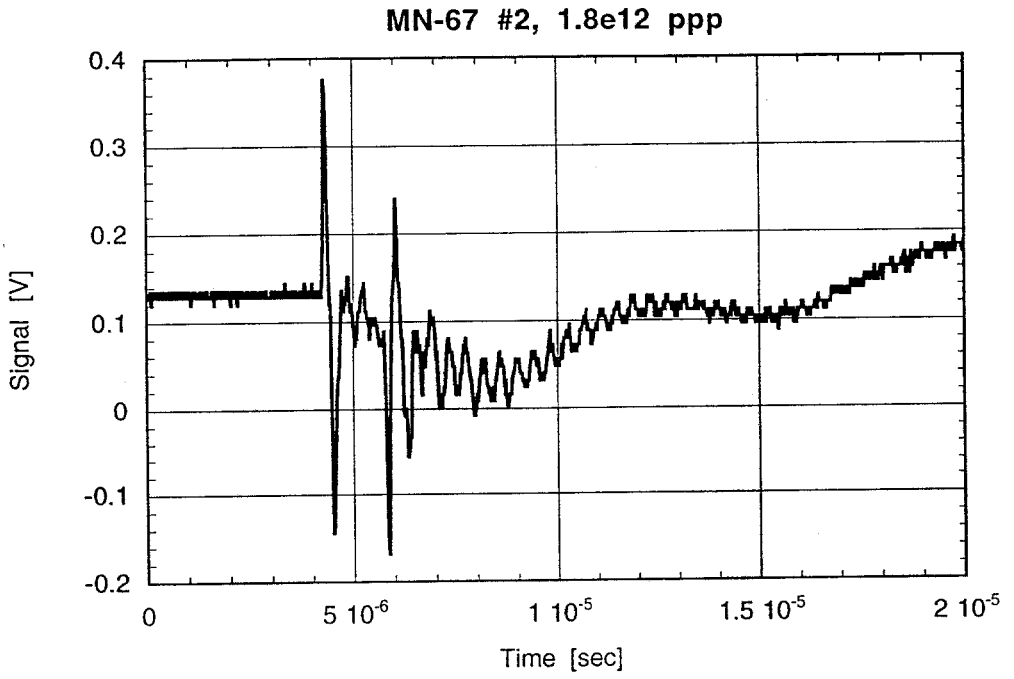
MN-67 #2, 1.8e12 ppp
Signal [V]
0.4
0.3
0.2
0.1
0
-0.1
-0.2
0
5 10-6
1 10-5
1.5 10-5
2 10-5
Time [sec]

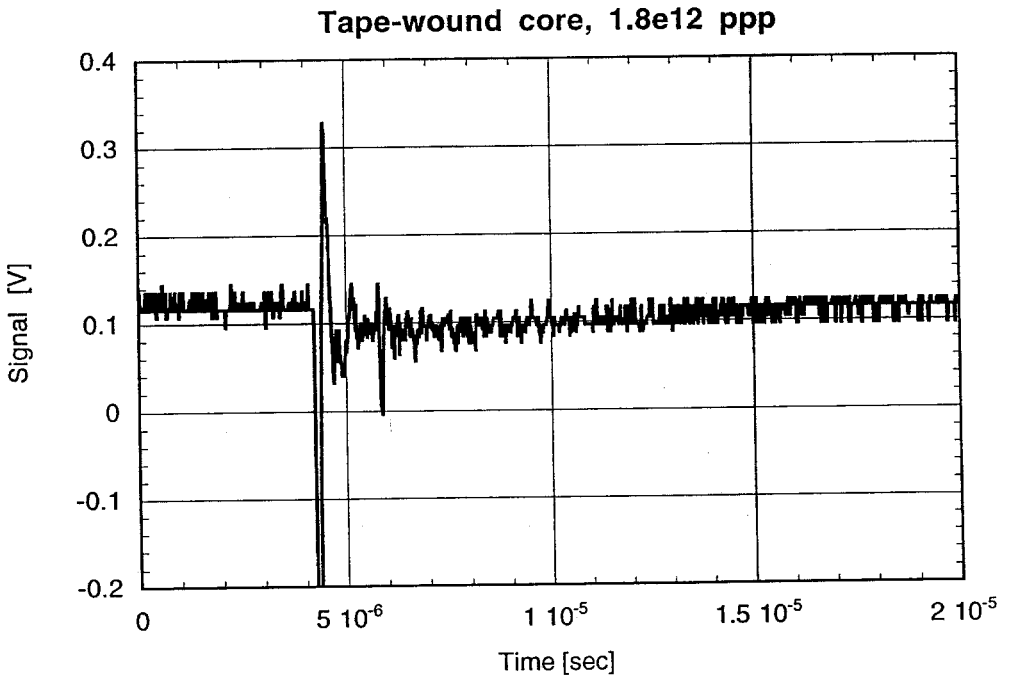
Tape-wound core, 1.8e12 ppp
Signal [V]
0.4
0.3
0.2
0.1
0
-0.1
-0.2
0
5 10-6
1 10-5
1.5 10-5
2 10-5
Time [sec]

Fig. 7